Energy Reports 7 (2021) 1162–1171

Contents lists available at ScienceDirect

Energy Reports

journal homepage: www.elsevier.com/locate/egyr

Effect of alcoholic and nano-particles additives on tribological properties of diesel–palm–sesame–biodiesel blends

M.A. Mujtaba [a,b,*], Haeng Muk Cho [c,**], H.H. Masjuki [a,d], M.A. Kalam [a,**], M. Farooq [b], Manzoore Elahi M. Soudagar [a], M. Gul [a,e], Waqar Ahmed [f], Asif Afzal [g], Shahid Bashir [h], V. Dhana Raju [i], Haseeb Yaqoob [j], A.Z. Syahir [a]

[a] Center for Energy Science, Department of Mechanical Engineering, University of Malaya, Kuala Lumpur 50603, Malaysia
[b] Department of Mechanical Engineering, University of Engineering and Technology, New Campus Lahore, Pakistan
[c] Division of Mechanical Engineering and Automotive Engineering, Kongju National University, 276, Budae-Dong, Cheonan-City, Chungnam, 330-717, South Korea
[d] Department of Mechanical Engineering, Faculty of Engineering, IIUM, 50728 Kuala Lumpur, Malaysia
[e] Department of Mechanical Engineering, Faculty of Engineering and Technology, Bahauddin Zakariya University, 60000 Multan, Pakistan
[f] Advanced CFD lab, Department of Mechanical Engineering, University of Malaya, Kuala Lumpur 50603, Malaysia
[g] Department of Mechanical Engineering, P. A. College of Engineering (Affiliated to Visvesvaraya Technological University, Belagavi), Mangaluru, 574153, India
[h] Department of Physics, Center of Ionics, Faculty of Science University of Malaya, Malaysia, Kuala Lumpur 50603, Malaysia
[i] Department of Mechanical Engineering, Lakireddy Bali Reddy College of Engineering, Mylavaram, Andhra Pradesh, 521230, India
[j] Khwaja Fareed University of Engineering and Information Technology, Rahim Yar Khan, Pakistan

ARTICLE INFO

Article history:
Received 19 January 2020
Received in revised form 17 November 2020
Accepted 7 December 2020
Available online 17 December 2020

Keywords:
Lubricity
Nanoparticles
Oxygenated alcohols
HFRR
Wear and Friction
Palm–sesame biodiesel

ABSTRACT

This study focused on evaluating the lubricity of diesel–biodiesel fuel with oxygenated alcoholic and nano-particle additives. Fuel injection system lubrication depended primarily on the fuel used in the diesel engine. Palm–sesame oil blend was used to produce biodiesel using the ultrasound-assisted technique. B30 fuel sample as a base fuel was blended with fuel additives in different proportions prior to tribological behavior analysis. The lubricity of fuel samples measured using HFRR in accordance with the standard method ASTM D6079. All tested fuels' Tribological behavior examined through worn steel balls and plates using scanning electron microscopy (SEM) to assess wear scar diameter and surface morphology. During the test run, the friction coefficient was measured directly by the HFRR tribometer system. The results exhibited that B10 (diesel) had a very poor coefficient of friction and wear scar diameter, among other tested fuels. The addition of oxygenated alcohol (ethanol) as a fuel additive in the B30 fuel sample decreased the lubricity of fuel and increased the wear and friction coefficient, among other fuel additives. B30 with DMC showed the least wear scar diameter among all tested fuels. B30 with nanoparticle TiO_2 exhibited the best results with the least wear scar diameter and lowest friction coefficient among all other fuel samples. B30+DMC demonstrated significant improvement in engine performance (BTE) and carbon emissions compared to different tested samples. B30+TiO_2 also showed considerable improvement in engine characteristics.

1. Introduction

Rapidly increased energy demand and stringent emission requirements attribute focus to renewable green biofuels from fossil fuels. Biodiesel is a potential candidate as an alternative fuel for compression ignition engines (Soudagar et al., 2020a; Ahmed et al., 2020). Due to poor cold flow properties, insufficient oxidation stability, poor fuel atomization, and higher NOx emissions, the biodiesel industry still faces problems in commercialization (Mujtaba et al., 2020d; Razzaq et al., 2020). Nowadays, biodiesel is blended with diesel fuel up to 30% in different regions of the world without any engine modification (Mujtaba et al.,

Abbreviations: CPO, Crude palm oil; CSO, Crude sesame oil; ASTM, American society for testing and materials; B10, commercial Malaysian diesel; B30, 70% diesel+30% biodiesel; EN, European; COF, coefficient of friction; WSD, wear scar diameter; TiO_2, titanium oxide; CNT, Carbon nano tubes; DMC, dimethyl carbonate; ULSD, Ultra-Low Sulfur Diesel; GC, Gas chromatography; FAME, Fatty acid methyl ester; HFRR, High frequency reciprocating rig; KOH, Potassium hydroxide; SEM, Scanning electron microscopy

* Corresponding author at: Center for Energy Science, Department of Mechanical Engineering, University of Malaya, Kuala Lumpur 50603, Malaysia.
** Corresponding authors.
E-mail addresses: m.mujtaba@uet.edu.pk (M.A. Mujtaba), haengmukcho@hanmail.net (H. Muk Cho), kalam@um.edu.my (M.A. Kalam).

https://doi.org/10.1016/j.egyr.2020.12.009

2020c). Indonesia and Malaysia produce biodiesel from palm oil in the region of Asia. Indonesia and Malaysia are using B20 and B10 biodiesel blends successfully, while B30 in Indonesia and the B20 in Malaysia will be introduced by 2020 (Elisha et al., 2019; Yusoff et al., 2020). Diesel–biodiesel blended fuel improved the engine emissions instead of NOx but, at the same time, decreased engine performance. Various researchers blending various fuel additives (nanoparticles or alcohols) to improve the Diesel–biodiesel blended fuel engine performance and engine emissions (Khan et al., 2020; Gavhane et al., 2020; Mujtaba et al., 2020a). Ultra-Low Sulfur Diesel (ULSD cleaner diesel) is produced with a maximum sulfur content of 15 ppm (Wadumesthrige et al., 2009). Diesel fuel's lubricity is crucial for engine components because injection systems and pumps are mainly lubricated by diesel fuel (Gul et al., 2020a). The lubricity of diesel fuel is reduced due to the elimination of polar compounds (polyaromatic and nitrogen) during the desulfurization process. These compounds produce a lubricating film (protective layer) between the metal mating surface to minimize wear and friction. High-pressure fuel injection systems can also reduce engine emissions, so fuel lubricity is key parameter to protect the injection system and other different engine components fuel lubricity (Lapuerta et al., 2010; Gul et al., 2020b).

Nowadays, researchers are blending fuel with nanoparticles like metal oxides of Al, Pt, Fe, Co, B, Ce, Ti, and Cu as an additive to improve engine performance and emission characteristics (Mujtaba et al., 2020b). Nonmetallic Graphene oxides (GO) and Carbon Nano Tubes (CNT's) blended with fuel as a prominent additive to enhance engine performance and emissions (Soudagar et al., 2018, 2019). Saxena et al. (2019) reported that TiO_2 showed better engine performance (thermal brake efficiency (BTE), brake specific fuel consumption (BSFC), and ignition delay (ID)) and emissions (hydrocarbons (HC) and smoke emissions). Among non-metal oxides, CNT's showed better engine performance and emissions results in comparison to diesel fuel. Zhang et al. (2019) Compared to cerium oxide and carbon nanotubes as an additive for engine testing, CNT nano additives exhibited better results in reducing engine emissions (NOx, PM, HC, and CO). El-Seesy and Hassan (2019) investigated engine performance and emissions by adding different non-metallic nanoparticles (graphene oxide, graphene nanoplatelets, and carbon nanotubes) with jatropha biodiesel–diesel blends. CNT's additive exhibited a significant reduction in specific fuel consumption and exhaust gas emissions (NOx, CO, and HC). Few researchers have also mixed CNT's nanoparticles with biodiesel–diesel fuel to improve the combustion efficiency, cetane number, and calorific value of fuel (Sadhik Basha and Anand, 2013; Alias et al., 2013; Balaji and Cheralathan, 2015). Various researchers (Şen, 2019; Lin et al., 2012; Fraioli et al., 2014; Pan et al., 2019; Atmanli, 2016; Liu et al., 2011; Soudagar et al., 2020b) also investigated the blending of different oxygenated alcoholic additives (butanol, pentanol, propanol, ethanol, di-ethyl ether, dimethyl carbonate, etc.) with Diesel–biodiesel blends for improvement of diesel engine performance and emissions. Venu (2019) researched to evaluate ethanol's influence (20%) with Diesel–biodiesel blends on engine performance and emissions. The results exhibited a reduction in exhaust gas emissions (NOx, CO, HC, and smoke emissions). Pan et al. (2019) conducted a research to investigate the effect of dimethyl carbonate coupled with exhaust gas recirculation method to minimize the engine exhaust emissions. Their research concluded that small amount of DMC up to 20% plays a vital role in reduction of 80% soot emissions. Dimethyl carbonate contains maximum amount of oxygen content among other oxygenated fuel additives.

Fuel lubricity is a crucial factor that should be controlled concerning the durability of diesel engine components. Many nations started to use ULSD (Ultra-Low Sulfur Diesel) to fulfill the Kyoto Protocol to minimize greenhouse gas emissions. ULSD has very poor lubricity in comparison to petroleum diesel. Desulfurization process reduced the sulfur content up to the minimum level (15 ppm), polar compounds, and other heteroatoms (oxygen and nitrogen compounds) from crude diesel (Farias et al., 2014). Due to insufficient lubrication provided ULSD fuel during fuel injection and pumping, engine parts become corroded or damaged. The addition of biodiesel in petroleum diesel significantly reduced the wear and friction due to the presence of 98% methyl ester content and other trace elements (monoglycerides, free glycerin, diglycerides, free fatty acids, antioxidants, tocopherols, vitamin E, etc.) (Wadumesthrige et al., 2009). By incorporating fuel additives, several experts have researched enhancing engine performance and emissions. It is also necessary that this additive effect on the lubricity of blended fuel or ternary fuel (diesel–biodiesel-additive) should also be evaluated prior to diesel engine testing.

This study evaluates the effect of fuel additives on the lubricity of Diesel–biodiesel blends (B30 as a base fuel) that were already proved good for enhancing the performance and emissions of the IC engines. Tribological behavior was observed for ternary blends (diesel–biodiesel-fuel additive) for the durability of diesel engines, pumps, and fuel injectors. According to the procedure described in ASTM, ternary fuel blends' lubricity is evaluated using HFRR (D6079-11). Palm–sesame oil blends were prepared to produce biodiesel. Palm and sesame oil mixed with a ratio of 50:50 to improve cold flow properties and oxidation stability. Sesame oil is mixed with palm oil prior to biodiesel production to improve palm oil's poor cold flow properties. Sesame oil exhibits excellent cold flow properties as well as oxidation stability, among other feedstocks. Sesame oil contains naturally occurring antioxidants. Sesame crop is cultivated in mostly Africa and Asia region. The United Republic of Tanzania is leading in the cultivation of sesame crops around the globe. The cost of low-quality sesame seeds is 0.64 $/kg, and sesame seed oil is 1.28 $/L (Mujtaba et al., 2020d).

In diesel engines, pumps and injectors are lubricated by diesel fuel itself during operation. Many researchers used different fuel additives (nanoparticles and oxygenated alcohols) to improve diesel engine performance and emission characteristics (Soudagar et al., 2018; Farias et al., 2014). Few researchers explored the effect of fuel additives on the lubricity of the fuel. The lubricity of fuel is a critical parameter related to the durability of diesel engines. Fuel additive's lubricity should be analyzed prior to engine testing. The lubricity of diesel injectors is crucial during the supply of diesel fuel in the combustion chamber. HFRR test is conducted with a ball-on-plate combination to analyze diesel fuel's lubricity with biodiesel and fuel additives mixture for fuel injector application. For this research work, ethanol and dimethyl carbonate has been chosen as an oxygenated distilled fuel additive and carbon nanotubes and titanium oxide as a nanoparticle additive. Scanning electron microscopy (SEM) tool utilized to analyze the plate and ball scars used in HFFR tests.

2. Materials and methods

2.1. Raw materials and chemicals

Crude palm oil (CPO) was taken from Sime Darby Plantation Berhad (Jomalina Refinery), Malaysia. Crude sesame oil (CSO) was sourced from the local market of Lahore, Pakistan. Methanol with purity 99.9% from Friendemann Schmidt, ACS, potassium hydroxide pellets (KOH) AR grade from Friendemann Schmidt, and Whatman filter papers Filtres Fioroni). Dehydrated Ethanol (purity: >99.5%) from Friendemann Schmidt, Dimethyl Carbonate

Table 1
FAME of P50S50 biodiesel produced from ultrasound-assisted technique.

Components of methyl esters (FAME: w/w%)	Carbon structure	Palm–sesame blend biodiesel P50S50
Methyl Myristate	C14:0	0.48
Methyl Palmitate	C16:0	24.59
Methyl Stearate	C18:0	4.45
Methyl Oleate	C18:1	42.48
Methyl Linoleate	C18:2	26.92
Methyl Linolenate	C18:3	0.49
Methyl Arachidate	C20:0	0.57
Total saturated		30.09
Total unsaturated		69.89

Table 2
Physicochemical properties of tested fuel samples.

Fuel samples	Physicochemical properties of fuel and its blends			
	Density kg/m^3	Viscosity mm^2/s	Viscosity index –	Calorific value MJ/kg
Standard specifications for pure biodiesel				
ASTM D6751 (Standard specifications) (Mujtaba et al., 2020d)	870–890	1.9–6.0	–	–
EN 14214 (Standard specifications) (Mujtaba et al., 2020d)	860–890	3.5–5.0	–	–
Tested fuel samples				
B10 (commercial diesel)	855.9	3.1507	81.2	44.1927
B100 (P50S50 biodiesel)	880.4	4.2110	186.2	40.2151
B30 (70% Diesel and 30% Biodiesel)	852.6	3.3189	164.2	43.4013
B30 + 20% (V/V) Dimethyl carbonate	878.0	2.0149	–	40.4611
B30 + 10% (V/V) Ethanol	847.0	3.0025	–	41.7887
B30 + Carbon Nano Tubes (100 ppm)	853.1	3.8064	176.8	43.075
B30 + TiO_2(100 ppm)	853.0	3.8606	208.3	44.006

Extra Dry (purity: 99+%) from Acros Organics and Nanoparticles (Carbon Nano Tubes and TiO_2) was taken from the chemistry department, University of Malaya. According to ASTM (D6079-11) dimensions, AISI 52100 Chrome hard polished steel balls with a diameter of 6.2 mm was purchased by SKF Malaysia Sdn Bhd, and 15 mm SAE-AMS 6440 steel smooth diamond polish disk was procured from the local market.

2.2. Biodiesel production

Ultrasound-assisted trans-esterified biodiesel produced from Palm–sesame oil blend with (50:50 blend ratio). Ultrasound-assisted trans-esterification was carried out under the following working conditions: methanol to oil ratio (9:1), time (40 min), catalyst concentration (1 wt%), and duty cycle (60%). When the transesterification reaction was completed, the reactor mixture was shifted to a funnel to separate methyl ester and glycerine with impurities. This mixture was left for 8 h settling time in the funnel. The lower layer containing glycerol was formed, while the upper layer contained biodiesel, catalyst, and excess methanol.

The lower layer was removed from the funnel by an opening stopcock. The upper layer containing catalyst and methanol content was washed with warm water (40 °C) until the clear water layer was found. Hot bubble washed methyl ester was shifted to the round bottom flask (500 ml) for further purification of methyl ester by removing water and methanol content using rotary evaporator equipment at 70 °C with rotational speed 150 rpm for 30 min. Lastly, evaporated biodiesel was filtered using the Whatman filter paper to eliminate the remaining trace amount of catalyst and stored in a vacuum chamber. The maximum optimal P50S50 predicted yield 96.138% was obtained using ELM coupling with cuckoo search optimization algorithm with optimum process variables: time (38.96 min), duty cycle (59.52%), methanol to oil ratio (60 V/V%), and catalyst (KOH) amount (0.70 Wt.%). The gas chromatography equipment (Agilent 7890, USA) was utilized for the fatty acid composition of P50S50 biodiesel, as shown in Table 1. Physicochemical properties of P50S50 biodiesel mentioned in Table 2.

2.3. Fuel sample preparation

Seven fuel samples were used to study the tribological behavior and lubricity of fuels. Commercial diesel (B10) was obtained from Shell, Malaysia, which was further used to compare other fuel samples results. B100 (P50S50 biodiesel) is produced at a lab scale. B30 (70% Diesel and 30% biodiesel) fuel sample is prepared by mixing 20% of biodiesel with commercially available diesel. Four fuel additive samples were ready to analyze their effect on the lubricity of fuel during fuel injection. B30 fuel is mixed with Dimethyl Carbonate (DMC) 20% by volume. Another alcoholic B30 fuel sample is prepared by mixing 10% Ethanol in volume. Ultrasonicated B30 with Carbon Nano-tubes (CNT) fuel sample is produced. Nanoparticle additive B30 with a TiO_2 fuel sample is prepared after ultrasonication. B30 and alcoholic fuel samples were prepared with 900 rpm stirring speed in 20 min. Nanoparticle additive fuel samples were prepared by mixing 5 mg of nanoparticle per 50 ml of B30 fuel with 20 mg of sodium dodecyl sulfate as a surfactant. B30 with nanoparticle and surfactant stirred at 900 rpm for 30 min and then sonicated for 10 min at pulse rate (3 s on and 2 s off) with 30% amplitude. Before tribological studies, seven fuel samples' physicochemical properties were measured like viscosity, viscosity index, and density (SVM 3000) and calorific value (C2000 basic calorimeter) in Table 2. QSONICA (Q500 Sonicate), which had a 20 kHz frequency with a maximum rated power of 500 W, was used for biodiesel production and preparation of nanoparticle fuel sample.

2.4. Tribological HFRR test

Seven fuel samples were evaluated using the High-Frequency Reciprocating Rig (HFRR) equipment from DUCOM (Model: TR-281-M8) shown in Fig. 1. The testing specimen plates were prepared by cutting 15 mm x15 mm pieces. The specimens were polished with 600, 800, 1000, 1500, and 2000 silicon carbide papers using the polishing machine. Then, the 3um and 1um diamond suspension were used for further polishing. The specimens' surface roughness was between 0.03 μm (Ra) and 0.04 μm (Ra).

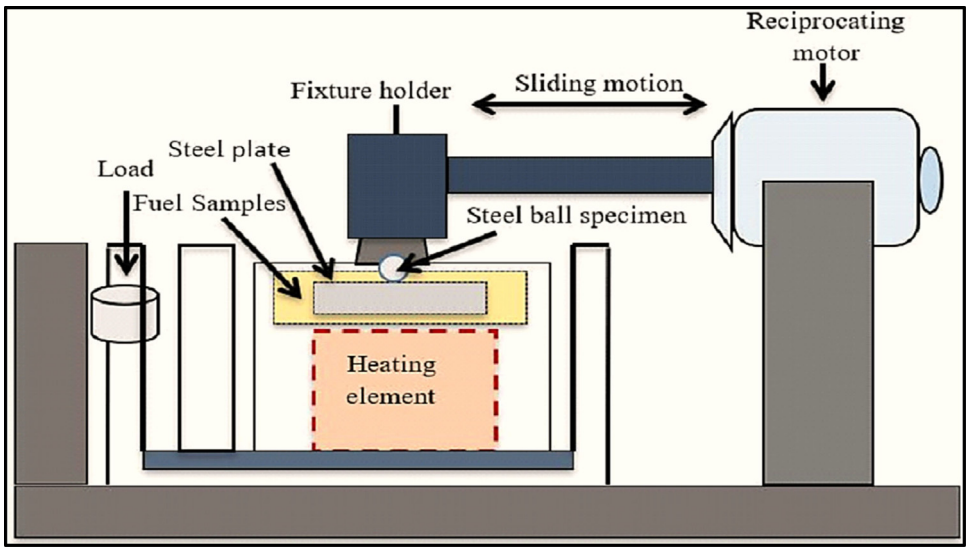

Fig. 1. Schematic diagram of Reciprocating Friction and Wear Monitor (HFRR) Rig.

Table 3
HFRR tribological test operating conditions.

Test parameters	Standard value
Sample temperature	60 °C
Sample test duration	70 min
Applied load	500 g
Frequency	10 Hz
Stroke length	2 mm
Sample volume	5 ml

The surface roughness of the specimens was measured by a profilometer (Veeco Dektak 150). A ball on a test specimen plate is performed to analyze the tribological behavior of fuel samples. A steel ball slides on a steel specimen plate submerged in 5.0 ± 0.2 ml fuel sample in a reciprocating motion with 2.0 ± 0.02 mm stroke length at a frequency 10.0 ± 1 Hz for 70 min with an applied load of 5 ± 0.01 N. Fuel temperature is constant at 60 ± 2 °C during the tribology test. All operating conditions were followed by standard test method ASTM D6079-11 and given in Table 3.

After tribological experiments, Scanning Electron Microscopy (SEM) was utilized to investigate the surface morphology and measure the wear scar diameter (WSD) of worn steel ball and steel plate. SEM images were captured at 2000 x and 3000 x magnification to visualize the nature of wear. The WSD of worn surfaces was calculated using the following equation WSD = (M + N)/2. In this equation, M represents the major axis, and N represents the minor axis (μm) measured through SEM. The coefficient of friction was measured by using the following equation:

$$\text{Coefficient of friction } (\mu) = \text{Actual frictional force (N)/Applied Load (N)}$$

3. Results and discussion

3.1. Tribological behavior: Coefficient of friction and wear scar diameter

Coefficient of friction trend for seven fuel samples illustrated in Fig. 2. The lubricity of diesel fuel is evaluated using a common standard test method (ASTM D6079-11) using the High-Frequency Reciprocating Rig (HFRR). The maximum allowable wear scar diameter measured by standard test method at 60 °C is 520 μm (ASTM D 975-10) and 460 μm (EN 590-10), according to American and European standards respectively (Farias et al., 2014). At the start of each experiment, the friction trend is unstable with respect to time known as the run-in period. After a few minutes, this friction trend starts to stabilize, known as the steady-state condition (Habibullah et al., 2015). It is seen from the friction trend that the un-steady state of B10 (Diesel) increases with time in comparison to other B30 fuel samples with additives. The presence of more percentage of ester content in biodiesel fuel samples provides a better protection layer as compared to B10 (Diesel) and B30 fuel sample. The presence of ester content in the fuel sample leads to the conversion of run in the period to steady-state conditions quickly (Konishi et al., 1996). The run-in period for pure P50S50 biodiesel is lowest due to ester molecules' adsorption existing in the biodiesel sample. In the case of B100 biodiesel, ester molecules of biodiesel stick to the metallic contact surface. Fatty acids methyl ester reacts with metallic surfaces and forms a protective layer between them. Which decreased the 'run-in period' for pure biodiesel. A similar trend can be seen in nanoparticle fuel samples; the presence of nanoparticles in fuel samples acts as a surfactant for two metallic contact surfaces. Ester molecules and nanoparticles' presence in fuel samples act as a surfactant for contact surfaces (Fazal et al., 2013). It can be deduced from Fig. 2; the friction coefficient decreases gradually with respect to time for all fuel samples except B100 and B30 + Eth fuel samples. The coefficient of friction for B100 and B30 + Eth increases up to 10 min and then sudden decrement in value with time. This phenomenon occurred due to the fatty acid composition of biodiesel like after the run-in period, fatty acids of B100 and B30 + Eth fuel samples were not involved in lubricant film formation until the period of 10 min after the development of a thin film layer resulting in a rapid reduction of the friction coefficient for B30 and B100 respectively (Zulkifli et al., 2013).

B10 (Diesel) has a higher average coefficient of friction (0.0676) and lower lubricity among other fuel samples due to the presence of higher Sulfur content. In diesel engines, fuel lubricity is important because it provides lubrication during rotating pumps and fuel injection (Barbour et al., 2000). B100 biodiesel and B30 fuel sample showed good lubricity and low coefficient of friction compared to alcoholic additives (B30 + DMC and B30 + Eth) and B10 (Diesel). The higher percentage of unsaturated fatty acids and long carbon chain fatty acids in biodiesel enhanced the lubricity of fuel and reduced the wear and friction between metallic contact surfaces. Another reason is

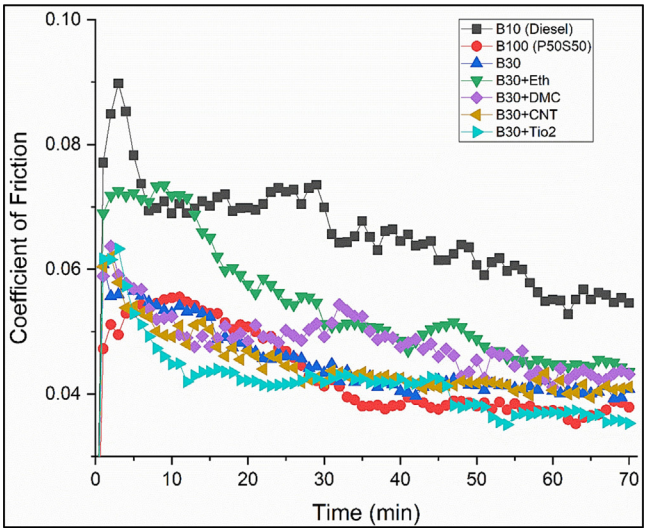

Fig. 2. Coefficient of friction trend with respect to time (min).

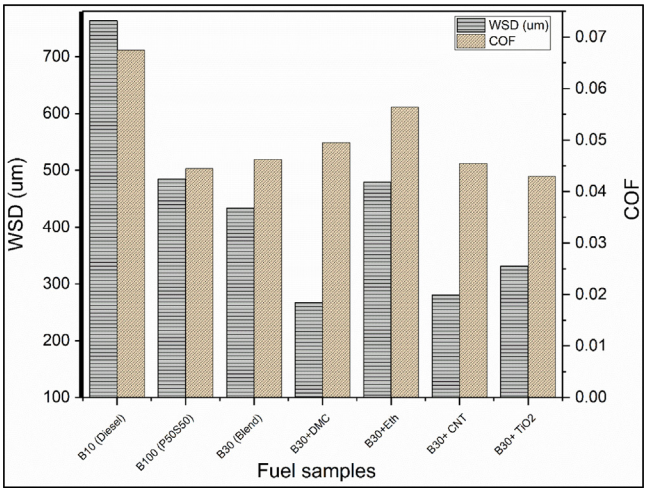

Fig. 3. Wear scar diameter and coefficient of friction of tested fuel samples.

that heteroatom lubricating film's uniform availability between mating surfaces also reduces the friction because heteroatom includes oxygen and Sulfur content. The kinematic viscosity of the B30 + Eth fuel sample is 3.0025 mm^2/s, as shown in Table 2. The B30 + Eth sample's lubricity is significantly affected due to lower density, which further hinders the formation of the lubricating thin film between ball-plate metallic contact. B30 fuel sample contains a low percentage of oxygen content, but the B30 + Eth fuel sample contains a high oxygen content rate due to high oxygenated alcohol (ethanol). The higher percentage of oxygen resulting in increased wear and friction coefficient due to oxidation of metallic surface can be seen from Fig. 3. A similar trend is reported by various researchers (Kuszewski et al., 2017; Lapuerta et al., 2010). Lower lubricity of ethanol B30 blend is mainly affected by following properties like volatility, temperature-sensitive, tribological behavior, and blending stability. The addition of ethanol up to 10% by volume resulted in a higher coefficient of friction, and wear scar diameter can be seen from Figs. 2 and 3. These results attributed that higher COF and WSD in the case of B30 + Eth was due to high evaporation rate of ethanol from lubricating film.

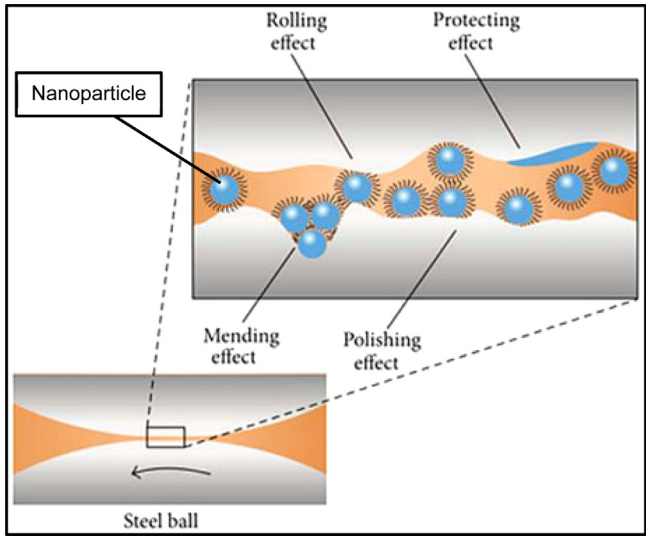

Fig. 4. Schematic diagram of the lubrication mechanism during the HFRR test with Nanoparticles (Gulzar, 2018).

B30 fuel blended with ethanol-fueled in compression ignition engine, which produced oxidation products during continuous flow through the injection system. These products removed the oxide layers from the injection system's moving components, and consequently, the anti-wear effects weaken. Similar increments in wear for diesel–ethanol blend were reported by other researchers (Chacartegui et al., 2007; Corkwell and Jackson, 2002). Dimethyl carbonate (DMC) as an oxygenated fuel additive blended with B30 showed promising WSD and COF results compared to B30 blended with ethanol. DMC contains a higher amount of oxygen content among all fuel samples. From Fig. 3, the WSD value for B30 + DMC is lowest among all fuel samples. The result can be attributed that at the start of the experiment, the anti-adhesive oxide layer is formed between metallic contact surfaces, which resulted in less wear and less WSD.

Nanoparticles combined with lubricants to improve their lubricity, wear, and friction. During this HFRR test, nanoparticles make a lubricating film between the metallic contacts. There are four different types of phenomena in the lubrication mechanism, like ball-bearing effect, protecting film formation, polishing, and mending impact, as shown in Fig. 4.

In this research work, Titanium oxide (TiO_2) and Carbon Nano Tubes (CNT's) were combined with a B30 fuel sample to investigate its effect on the lubricity of fuel for injection system application. B30 + TiO_2 fuel sample showed the least friction coefficient (0.0430) among all other fuel samples, followed by B100 (P50S50). From Fig. 3, B30 + TiO_2 exhibited better anti-wear behavior and reduced coefficient of friction. This result attributed the formation of effective and uniform lubricating thin TiO_2 film between metallic surface contact (ball to plate). Other researchers also reported the significance of nano-TiO_2 in reducing the friction coefficient of mineral lubricant (Shahnazar et al., 2016; Wu et al., 2007; Arumugam and Sriram, 2013; Ingole et al., 2013). Similarly, the above-mentioned experimental results support the addition of TiO_2 in fuels to enhance its lubricity for fuel injectors.

B30 + CNT fuel sample showed better tribological properties (WSD and COF) among all other fuel samples instead of B30 + TiO_2. B30 + CNT fuel sample exhibited the lowest WSD due to the formation of lubricating thin CNT anti-adhesive film between contact surfaces. COF of the B30 + CNT fuel sample is higher than B30 + TiO_2 due to particles' agglomeration in the fuel sample. The dispersion of CNT's in the fuel sample is quite challenging due to CNT's chemical inert behavior (Shahnazar et al., 2016).

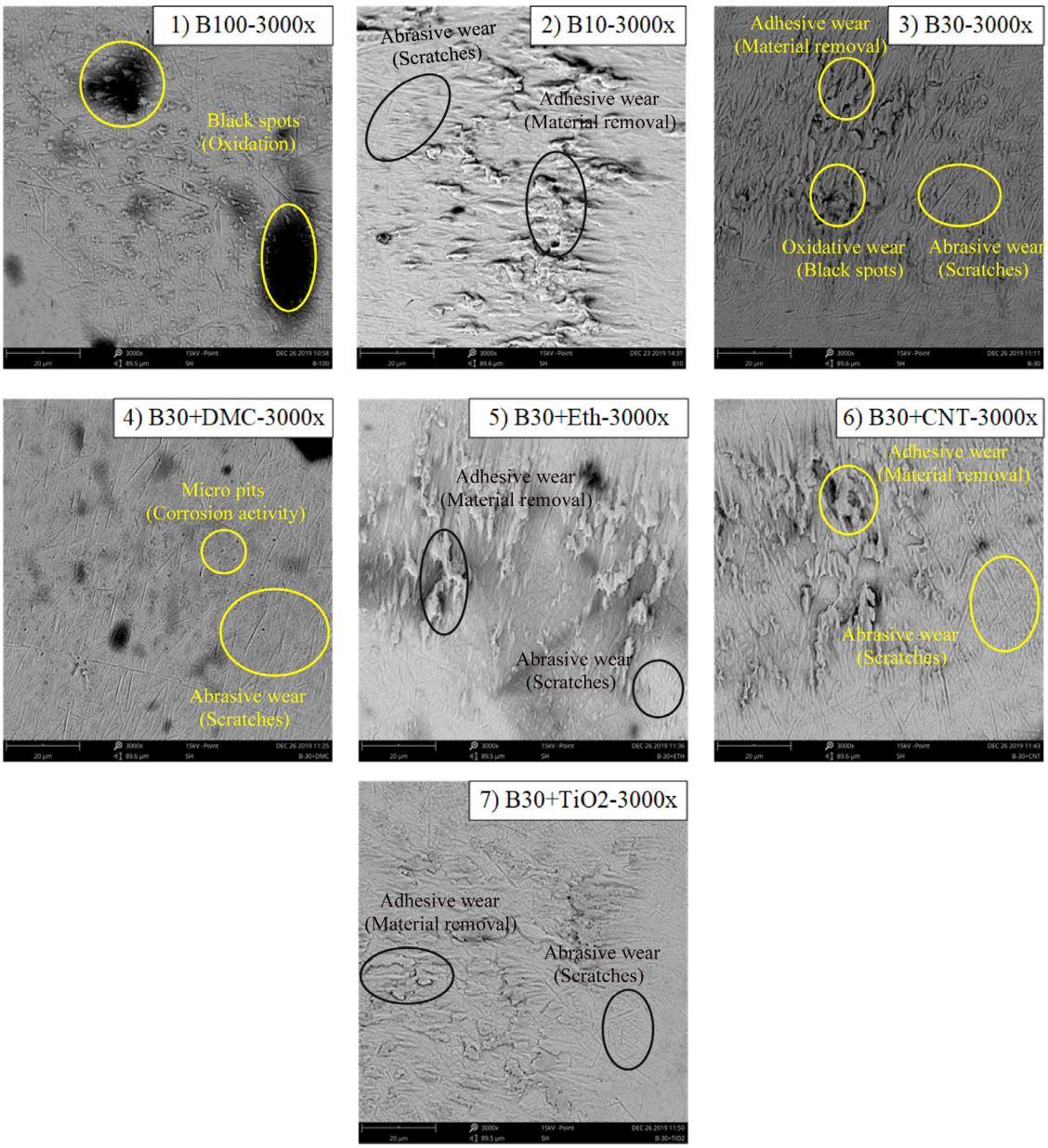

Fig. 5. SEM micrographs of worn steel ball used in HFRR test magnified at 3000x.

Lubricating thin films' stability between metallic mating surfaces depends on the fuel's fatty acid composition, fluid viscosity, temperature, dispersion of Nano-additives in fuel, applied load, and speed (Maleque et al., 2000). Oxidation phenomenon transforms ester into different fatty acids (propionic acid, formic acid, acetic acid, etc.) that increase fuel lubricity. Still, sometimes it becomes corrosive for diesel engine components (pump and injection system) (Maleque et al., 2000; Sulek et al., 2010; Anastopoulos et al., 2001). Length of carbon chain molecules, degree of unsaturation (presence of double and triple bonds), oxygen content in biodiesel, nanoparticle additives, and oxygenated alcoholic additives play an important role in enhancing the lubricity of the fuel. Impurities, in the form of monoglycerides, diglycerides, and free fatty acids in biodiesel, also contributed to the lubricity improvement (Hu et al., 2005).

3.2. SEM analysis

3.2.1. Morphological study of worn steel ball

Fig. 5 shows the micrographs of worn steel balls used for various fuel samples during the HFRR test to visualize wear behavior. Major surface deformation can be visualized from micrographs of B10, B30, B30 + Eth, and B30 + CNT. It is observed that particles detached from the cavities of worn steel balls of B10, B30, B30 + Eth, B30 + CNT, and B30 + TiO_2 are much bigger than 20 μm, which attributed to adhesive wear. The particles detached from the surface of B100 and B30 + DMC worn steel balls are lower than 20 μm (abrasive wear). The removal of larger particles of more than 20 μm from surface cavities known as adhesive wear (Rabinowicz, 1984). The small particles detached from worn surfaces lower than 20 μm reflecting towards abrasive wear (Sperring and Nowell, 2005). Fig. 5 (1) B100 shows that Black spots can be seen, predicting the oxidation phenomena. It will demonstrate the presence of oxygen content, which will help to form a lubricating film between mating surfaces due to the

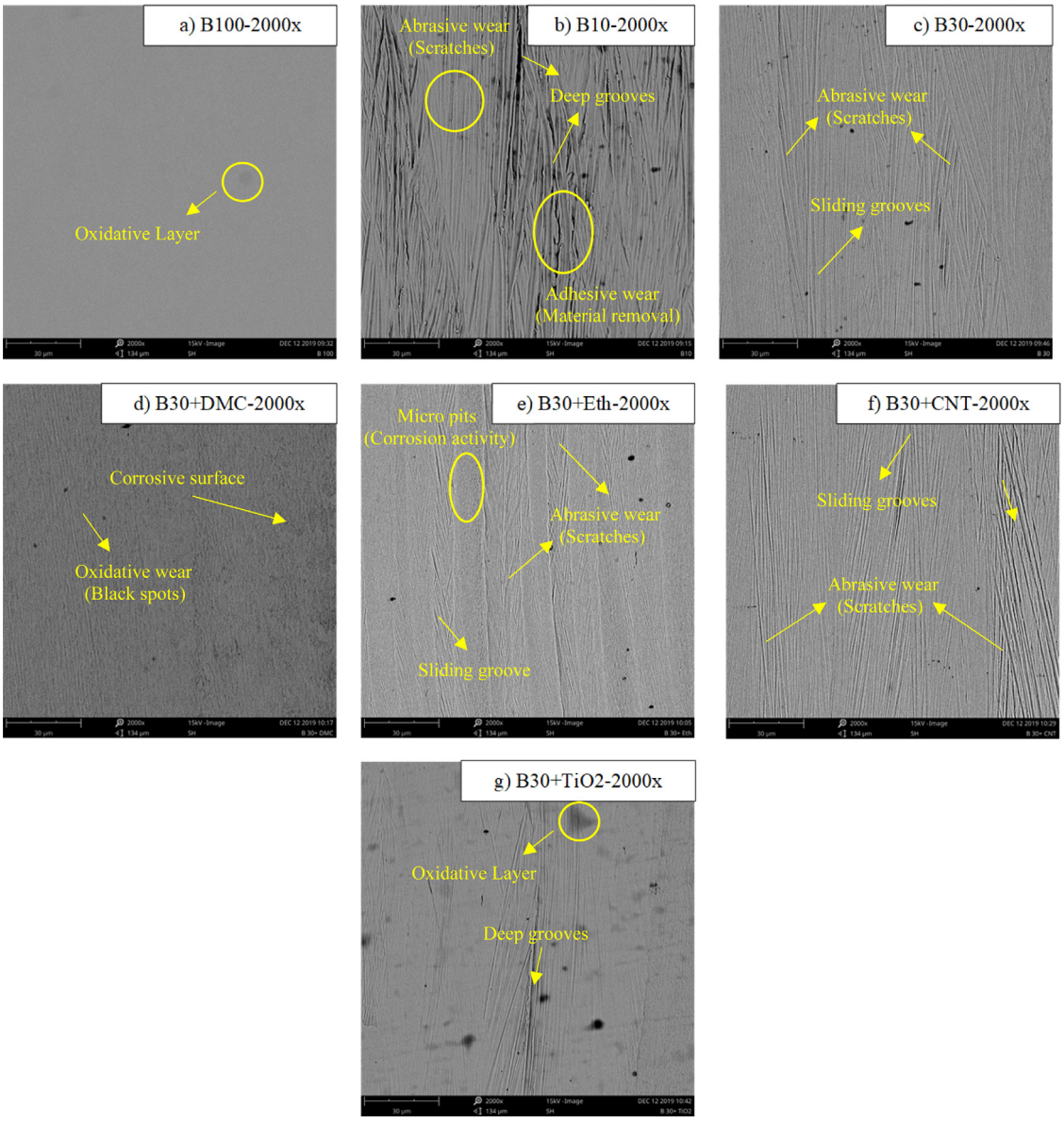

Fig. 6. SEM micrographs of worn steel plate used in HFRR test magnified at 2000x.

conversion of Fe_3O_4 and Fe_2O_3 inorganic oxides (Zulkifli et al., 2013). In B10 (Diesel), severe adhesive wear can be seen due to large particles' detachment from the worn surface.

Abrasive wear can also be visualized in the form of scratches. From Fig. 5 (3,5,6,7), the extrusion of small metal can be seen in the form of adhesive wear. Micro pits and corrosion activity can be visualized in the case of B30 + DMC and B30. As a result, oxidative corrosion is occurred in the form of corrosive wear due to the formation of different peroxides and acids during oxidation.

3.2.2. Morphological study of worn steel plate

Fig. 6 showed the surface morphology of worn surface plates. The micrograph of B100 depicts the oxidation process, which provides a lubricating film between rubbing surfaces. This result is attributed to oxygen content, double bonds, and a long chain of carbon atoms in biodiesel. This oxidative layer formed and removed continuously due to sliding motion, therefore giving a smooth surface. But with time, these removed unreactive detergents cause an increase in wear.

Deep grooves and scratches can be observed in the case of B10 (Diesel). This result is attributed to the erratic friction coefficient behavior and lack of lubricating thin film between rubbing metallic surfaces. Small sliding grooves, micro pitting due to corrosion activity in case of B30 + Eth fuel sample. The B30 + DMC surface's micrograph shows a corrosive surface due to a chemical attack on the plate's surface. This result is attributed to oxidative wear and metallic soap formation due to metallic surface reaction with the chemical. Oxidation can be seen in B30 + TiO2, which provides lubricating film between mating surfaces and reduces the overall coefficient of friction. Few deep grooves were also observed due to rubbing of debris and lead to adhesive wear.

3.3. Engine performance and emission characteristics

Fig. 7 exhibited the engine performance characteristics (BTE and BSFC) at full load engine conditions. TiO_2 and DMC were tested as fuel additives with diesel–biodiesel fuel blends due to better tribological behavior, among other fuel additives. The average BSFC values are 0.421, 0.442, 0.45 and 0.46 kg/kWh for B30 + TiO_2, B30 + DMC, B10 and B30, respectively. Ternary fuel

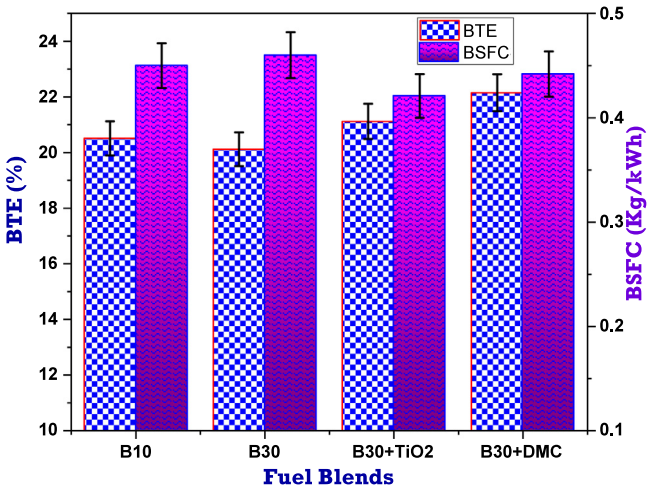

Fig. 7. BTE and BSFC trend for all fuel blends at full load condition.

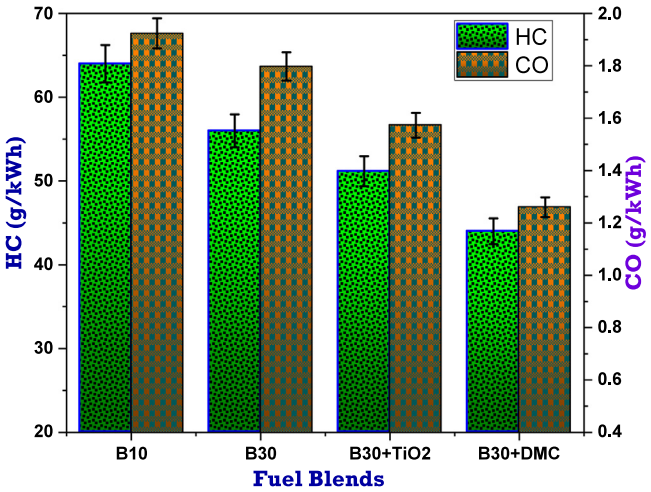

Fig. 8. The trend of carbon emissions (HC and CO) for fuel blends at full load condition.

blends showed a significant reduction in BSFC values of 8.48% and 3.91% for B30 + TiO_2 and B30 + DMC compared to B30 fuel.

The reduction in BSFC in nanoparticle ternary fuel blends due to lower ignition delay time resulted in less premixed combustion of fuel and air mixture (Nadeem et al., 2006). Oxygenated alcohol as a fuel additive showed a promising reduction in BSFC value due to lower viscosity and dimethyl carbonate density, which helped improve fuel spray characteristics, resulting in enhanced combustion performance (Imtenan et al., 2015; Soudagar et al., 2021). The average BTE values are 22.15, 21.12, 20.51 and 20.12% for B30 + DMC, B30 + TiO_2, B10 and B30, respectively. Ternary fuel blends showed a promising increase in the thermal efficiency of 10.09% and 4.97% for B30 + DMC and B30+ TiO2 due to high oxygen content. Oxygenated alcohols improved the BTE due to a high amount of oxygen content, which helped in better combustion and lower combustion time (Khalife et al., 2017). Fuel additives provide the excess oxygen in the fuel-rich zone during combustion in the combustion chamber, which resulted in improved combustion; consequently, BTE is increased compared to B30 fuel. B30 fuel showed very less BTE and brake power due to high viscosity compared to other fuel blends which resulted in poor atomization due to poor fuel spray characteristics. TiO_2 as a fuel additive act as a combustion catalyst due to its chemical reactive surface with excess oxygen, which resulted in enhanced combustion; consequently, BTE is increased (Saxena et al., 2019). Örs et al. (2018) also reported a significant reduction in BSFC 27.73% for B20 fuel with the addition of TiO_2 compared to B20 fuel. Yuvarajan Devarajan found a significant reduction in BSFC 4.1% and increased BTE 1.6% with DMC's addition as a fuel additive.

Fig. 8 showed the carbon emissions (HC and CO) trend at full load conditions. HC and CO emissions reduced for all fuel blends compared to commercial diesel (B10). CO emissions are produced due to incomplete combustion or partial combustion. The higher concentration of biodiesel in diesel–biodiesel fuel blends resulted in lower carbon emissions due to excess oxygen content, which improved the combustion process. CO emissions vary according to the combustion chamber's air-to-fuel ratio (Habibullah et al., 2014). The average CO emissions are 1.26, 1.57, 1.79, and 1.92 g/kWh for B10, B30, B30 + TiO_2, and B30 + DMC, respectively.

All ternary fuel blends showed a significant reduction in CO emissions compared to B10 due to higher combustion temperature in the combustion chamber. The conversion to CO_2 increased due to higher combustion temperature because of excess oxygen (higher air–fuel ratio) provided by fuel additives during the combustion process. On average, ternary fuel blends, including B30, showed a promising reduction of 6.57%, 18.22%, and 34.51% for B30, B30 + TiO_2, and B30 + DMC, respectively compared to B10 (commercial diesel). Alcoholic ternary fuel blends exhibited high CO emissions reduction due to the presence of a higher percentage of oxygen content in its molecular structure, which helped convert CO to CO2 and enhance the combustion process (Imtenan et al., 2014). Nanoparticle blended fuel also exhibited a significant reduction in CO emissions compared to B30 due to the presence of oxygen content, high chemical reactive surface, and larger surface area for the better combustion process, which resulted in a complete conversion of CO to CO_2.

HC emissions are produced due to an incomplete combustion process (Marikatti et al., 2020). All ternary fuel blends showed a promising reduction in HC emissions compared to B30 and B10 due to higher oxygen content and higher cetane number, which resulted in lower ignition delay (Anand et al., 2010). On average, HC emissions are 64, 56, 51, and 44 g/kWh for B10, B30, B30 + TiO_2, and B30 + DMC, respectively. On average, there is a significant reduction in HC emissions 12.5%, 20.06%, and 31.25% for B30, B30 + TiO_2, and B30 + DMC compared to B10 (commercial diesel). Alcoholic ternary fuel blends showed a noticeable reduction in HC emissions due to peak in-cylinder temperature and pressure, resulting in an improved and complete combustion process (Pan et al., 2019). Nanoparticle ternary fuel blends also showed a significant reduction in HC emissions due to the accelerated oxidation process for conversion of HC to water or CO2 provided by nanoparticles, resulting in lower HC emissions (Kalam and Masjuki, 2008).

4. Conclusion

This tribological study mainly focused on the lubricity of diesel fuel during injection applications in diesel engines. All diesel fuel samples are tested using HFRR equipment to evaluate diesel fuel lubricity compliance with the protocol set out in ASTM standard D6079-11. After the experimental investigation, WSD, COF, and microscopic images of SEM for B10 (Diesel) depict inferior results compared to other fuel samples. On average all fuel samples showed significant reduction in coefficient of friction 34.03%, 31.47%, 26.6%, 16.37%, 32.61% and 36.25% for B100, B30, B30 + DMC, B30 + Eth, B30 + CNT and B30 + TiO_2 respectively compared to B10 (commercial diesel). Among ternary fuel blends,

B30 + TiO_2 showed a promising reduction in COF due to titanium nanoparticles ball-bearing effect during rubbing of metallic surfaces. B10 (commercial diesel) exhibited very poor COF and WSD results compared to other tested fuel samples. These poor results attributed the un-steady state coefficient of friction with running time due to weak lubricating film between two metallic rubbing surfaces (ball to plate). The coefficient of friction is improved for all other fuel samples due to unsaturated fatty acids, oxygen content, and a trace amount of free fatty acid content in biodiesel. Ethanol blended fuel samples showed very high wear and coefficient of friction in comparison to other additives. During the test, the loss of ethanol evaporation results in weakening lubrication film formation between mating surfaces. Dimethyl carbonate blended fuel samples exhibited better results in comparison to ethanol. Its wear scar diameter is very less among all tested fuel samples due to the anti-adhesive lubricating film's formation at the beginning of the experiment due to high oxygen content in the fuel sample. Oxidative wear can also be seen from SEM images in the case of B30 + DMC due to chemical attacks on the metallic plate surface. Nanoparticles blended fuel samples showed the best tribological behavior among all tested fuel samples. Both wear and coefficient of friction are reduced due to the formation of lubricating nanoparticle thin film between metallic contact surfaces. Nanoparticles act as a sacrificial layer between metallic rubbing contact. The friction coefficient for the B30 + CNT fuel sample is high compared to the TiO_2 blended fuel sample. Addition of nanoparticles in B30 diesel–palm–sesame–biodiesel blends showed better tribological properties, among other all fuel additives. Dimethyl carbonate exhibited better wear and friction coefficient among alcoholic additives for diesel engines. B30 + DMC exhibited very promising diesel engine performance and emission results compared to other tested samples due to higher oxygen content. B30 + TiO_2 also improved diesel engine characteristics compared to B30 fuel.

It is concluded that the addition of nanoparticles like TiO_2 and alcohol like dimethyl carbonate in B30 diesel–palm–sesame–biodiesel fuel is good for the durability of diesel engines, pumps, and fuel injectors because these additives improve the lubricity of the B30 fuel.

CRediT authorship contribution statement

M.A. Mujtaba: Conceptualization, Investigation, Writing - original draft. **Haeng Muk Cho:** Funding acquisition. **H.H. Masjuki:** Supervision. **M.A. Kalam:** Supervision, Project administration. **M. Farooq:** Review & Editing. **Manzoore Elahi M. Soudagar:** Conceptualization, Review and Editing, Analysis. **M. Gul:** Data Curation, Formal analysis, Review & Editing. **Waqar Ahmed:** Review & Editing. **Asif Afzal:** Review & Editing. **Shahid Bashir:** Review & Editing. **V. Dhana Raju:** Software. **Haseeb Yaqoob:** Software. **A.Z. Syahir:** Validation.

Declaration of competing interest

The authors declare that they have no known competing financial interests or personal relationships that could have appeared to influence the work reported in this paper.

Acknowledgments

This work was supported by the National Research Foundation of Korea (NRF) grant funded by the Korea government (MSIT) (NRF-2019R1A2C1010557). The authors would also like to thank the University of Malaya for supporting Ph.D. students through research grant GPF018A-2019.

References

Ahmed, Waqar, et al., 2020. Ultrasonic assisted new Al2O3@ TiO2-ZnO/DW ternary composites nanofluids for enhanced energy transportation in a closed horizontal circular flow passage. Int. Commun. Heat Mass Transfer 105018.

Alias, A., Thegaraju, D., Sharma, K., 2013. Effect of carbon nanotube dispersions to the palm oil diesel–biodiesel blend properties, Conference Effect of Carbon Nanotube Dispersions to the Palm Oil Diesel–Biodiesel Blend Properties, Vol. 1, p. 3.

Anand, R., Kannan, G., Nagarajan, S., Velmathi, S., 2010. Performance Emission and Combustion Characteristics of a Diesel Engine Fueled with Biodiesel Produced from Waste Cooking Oil. SAE technical paper.

Anastopoulos, G., Lois, E., Serdari, A., Zanikos, F., Stournas, S., Kalligeros, S., 2001. Lubrication properties of low-sulfur diesel fuels in the presence of specific types of fatty acid derivatives. 15 (1), 106–112.

Arumugam, S., Sriram, G., 2013. Preliminary study of nano-and microscale TiO2 additives on tribological behavior of chemically modified rapeseed oil. Tribol. Trans. 56 (5), 797–805.

Atmanli, A., 2016. Comparative analyses of diesel–waste oil biodiesel and propanol, n-butanol or 1-pentanol blends in a diesel engine. Fuel 176, 209–215.

Balaji, G., Cheralathan, M., 2015. Effect of CNT as additive with biodiesel on the performance and emission characteristics of a DI diesel engine. 7 (3), 1230–1236.

Barbour, R.H., Rickeard, D.J., Elliott, N.G., 2000. Understanding Diesel Lubricity. SAE International.

Chacartegui, C., Lopez, J., Alfonso, F., Aakko, P., Hamelinck, C., Vossen, G., et al., 2007. Blending ethanol in diesel. In: Final Report for Lot 3b of the Biodiesel Improvement on Standards, Coordination of Producers Ethanol Studies Project.

Corkwell, K.C., Jackson, M.M., 2002. Lubricity and Injector Pump Wear Issues with E Diesel Fuel Blends. SAE Technical Paper.

El-Seesy, A.I., Hassan, H., 2019. Investigation of the effect of adding graphene oxide, graphene nanoplatelet, and multiwalled carbon nanotube additives with n-butanol-Jatropha methyl ester on a diesel engine performance. Renew. Energy 132, 558–574.

Elisha, O., Fauzi, A., Anggraini, E., 2019. Analysis of Production and Consumption of Palm-Oil Based Biofuel using System Dynamics Model: Case of Indonesia.

Farias, A.C.M.d., Medeiros, J.T.N.d., Alves, S.M., 2014. Micro and nanometric wear evaluation of metal discs used on determination of biodiesel fuel lubricity. 17, 89–99.

Fazal, M.A., Haseeb, A.S.M.A., Masjuki, H.H., 2013. Investigation of friction and wear characteristics of palm biodiesel. Energy Convers. Manage. 67, 251–256.

Fraioli, V., Mancaruso, E., Migliaccio, M., Vaglieco, B.M., 2014. Ethanol effect as premixed fuel in dual-fuel CI engines: experimental and numerical investigations. Appl. Energy 119, 394–404.

Gavhane, S.R., Kate, M.A., Pawar, A., Safaei, M.R., Soudagar, M.M.E., Mujtaba Abbas, M., et al., 2020. Effect of zinc oxide nano-additives and soybean biodiesel at varying loads and compression ratios on VCR diesel Engine Characteristics. Symmetry 12 (6), 1042.

Gul, M., Masjuki, H.H., Kalam, M.A., Zulkifli, N.W.M., Mujtaba, M.A., 2020a. A review: Role of fatty acids composition in characterizing potential feedstock for sustainable green lubricants by advance transesterification process and its global as well as Pakistani prospective. BioEnergy Res. 13 (1), 1–22.

Gul, M., Zulkifli, N., Masjuki, H., Kalam, M., Mujtaba, M., Harith, M., et al., 2020b. Effect of TMP-based-cottonseed oil-biolubricant blends on tribological behavior of cylinder liner-piston ring combinations. Fuel 278, 118242.

Gulzar, M., 2018. Tribological Study of Nanoparticles Enriched Bio-Based Lubricants for Piston Ring–Cylinder Interaction. Springer.

Habibullah, M., Masjuki, H.H., Kalam, M.A., Fattah, I.M.Rizwanul., Ashraful, A.M., Mobarak, H.M., 2014. Biodiesel production and performance evaluation of coconut, palm and their combined blend with diesel in a single-cylinder diesel engine. Energy Convers. Manage. 87, 250–257.

Habibullah, M., Masjuki, H.H., Kalam, M.A., Zulkifli, N.W.M., Masum, B.M., Arslan, A., et al., 2015. Friction and wear characteristics of Calophyllum inophyllum biodiesel. Ind. Crops Prod. 76, 188–197.

Hu, J., Du, Z., Li, C., Min, 2005. Study on the lubrication properties of biodiesel as fuel lubricity enhancers. 84 (12-13), 1601–166.

Imtenan, S., Masjuki, H.H., Varman, M., Fattah, I.R.J.R.A., 2015. Evaluation of n-butanol as an oxygenated additive to improve combustion-emission-performance characteristics of a diesel engine fuelled with a diesel-calophyllum inophyllum biodiesel blend. 5 (22), 17160–17170.

Imtenan, S., Masjuki, H., Varman, M., Kalam, M., Arbab, M., Sajjad, H., et al., 2014. Impact of oxygenated additives to palm and jatropha biodiesel blends in the context of performance and emissions characteristics of a light-duty diesel engine. 83, 149–158.

Ingole, S., Charanpahari, A., Kakade, A., Umare, S., Bhatt, D., Menghani, J., 2013. Tribological behavior of nano TiO2 as an additive in base oil. Wear 301 (1–2), 776–785.

Kalam, M., Masjuki, H.J.B., 2008. Testing palm biodiesel and NPAA additives to control NOx and CO while improving efficiency in diesel engines. Bioenergy 32 (12), 1116–1122.

Khalife, E., Tabatabaei, M., Demirbas, A., Aghbashlo, M.J.P.iE., Science, C., 2017. Impacts of additives on performance and emission characteristics of diesel engines during steady state operation. 59, 32–78.

Khan, H., Soudagar, M.E.M., Kumar, R.H., Safaei, M.R., Farooq, M., Khidmatgar, A., et al., 2020. Effect of nano-graphene oxide and n-Butanol fuel Additives Blended with Diesel—Nigella sativa biodiesel fuel emulsion on diesel engine characteristics. Symmetry 12 (6), 961.

Konishi, T., Klaus, E.E., Duda, J.L., 1996. Wear characteristics of Aluminum-Silicon Alloy under Lubricated Sliding Conditions. Tribol. Trans. 39 (4), 811–818.

Kuszewski, H., Jaworski, A., Ustrzycki, A., 2017. Lubricity of ethanol–diesel blends – Study with the HFRR method. Fuel 208, 491–498.

Lapuerta, M., García-Contreras, R., Agudelo, J.R., 2010. Lubricity of ethanol-biodiesel-diesel fuel blends. Energy Fuels 24 (2), 1374–1379.

Lin, S.-L., Lee, W.-J., Lee, C.-fF., Wu, Y.-p., 2012. Reduction in emissions of nitrogen oxides, particulate matter, and polycyclic aromatic hydrocarbon by adding water-containing butanol into a diesel-fueled engine generator. Fuel 93, 364–372.

Liu, H., Lee, C.-f., Huo, M., Yao, M., 2011. Comparison of ethanol and butanol as additives in Soybean biodiesel using a constant volume Combustion Chamber. Energy Fuels 25 (4), 1837–1846.

Maleque, M.A., Masjuki, H.H., Haseeb, A., 2000. Effect of mechanical factors on tribological properties of palm oil methyl ester blended lubricant. Wear 239 (1), 117–125.

Marikatti, Mahantesh, Banapurmath, N.R., Yaliwal, V.S., Basavarajappa, Y.H., Soudagar, Manzoore Elahi M., García Márquez, Fausto Pedro, Mujtaba, M.A., et al., 2020. Hydrogen injection in a dual fuel engine fueled with low-pressure injection of Methyl Ester of Thevetia Peruviana (METP) for diesel engine maintenance application. Energies 13 (21), 5663.

Mujtaba, M., Kalam, M., Masjuki, H., Gul, M., Soudagar, M.E.M., Ong, H.C., et al., 2020a. Comparative study of nanoparticles and alcoholic fuel additives-biodiesel-diesel blend for performance and emission improvements. Fuel 279, 118434.

Mujtaba, M., Masjuki, H., Kalam, M., Noor, F., Farooq, M., Ong, H.C., et al., 2020b. Effect of additivized biodiesel blends on diesel engine performance, emission, tribological characteristics, and Lubricant Tribology. Energies 13 (13), 3375.

Mujtaba, M., Masjuki, H., Kalam, M., Ong, H.C., Gul, M., Farooq, M., et al., 2020c. Ultrasound-assisted process optimization and tribological characteristics of biodiesel from palm-sesame oil via response surface methodology and extreme learning machine-Cuckoo search. Renew. Energy.

Mujtaba, M.A., Muk Cho, H., Masjuki, H.H., Kalam, M.A., Ong, H.C., Gul, M., et al., 2020d. Critical review on sesame seed oil and its methyl ester on cold flow and oxidation stability. Energy Rep. 6, 40–54.

Nadeem, M., Rangkuti, C., Anuar, K., Haq, M., Tan, I., Shah, S.J.F., 2006. Diesel engine performance and emission evaluation using emulsified fuels stabilized by conventional and gemini surfactants. 85 (14-15), 2111–2119.

Örs, I., Sarıkoç, S., Atabani, A., Ünalan, S., Akansu, S.J.F., 2018. The effects on performance, combustion and emission characteristics of DICI engine fuelled with TiO2 nanoparticles addition in diesel/biodiesel/n-butanol blends. 234, 177–188.

Pan, M., Qian, W., Zheng, Z., Huang, R., Zhou, X., Huang, H., et al., 2019. The potential of dimethyl carbonate (DMC) as an alternative fuel for compression ignition engines with different EGR rates. Fuel 257, 115920.

Rabinowicz, E., 1984. The least wear. Wear 100 (1–3), 533–541.

Razzaq, L., Farooq, M., Mujtaba, M., Sher, F., Farhan, M., Hassan, M.T., et al., 2020. Modeling viscosity and density of ethanol-diesel-biodiesel ternary blends for sustainable environment. Sustainability 12 (12), 5186.

Sadhik Basha, J., Anand, R.B., 2013. The influence of nano additive blended biodiesel fuels on the working characteristics of a diesel engine. J. Braz. Soc. Mech. Sci. Eng. 35 (3), 257–264.

Saxena, V., Kumar, N., Saxena, V.K., 2019. Multi-objective optimization of modified nanofluid fuel blends at different TiO2 nanoparticle concentration in diesel engine: Experimental assessment and modeling. Appl. Energy 248, 330–353.

Şen, M., 2019. The effect of the injection pressure on single cylinder diesel engine fueled with propanol–diesel blend. Fuel 254, 115617.

Shahnazar, S., Bagheri, S., Abd Hamid, S.B., 2016. Enhancing lubricant properties by nanoparticle additives. Int. J. Hydrogen Energy 41 (4), 3153–3170.

Soudagar, Manzoore Elahi M., Afzal, Asif, Safaei, Mohammad Reza, Manokar, A. Muthu, EL-Seesy, Ahmed I., Mujtaba, M.A., Samuel, Olusegun David, et al., 2020a. Investigation on the effect of cottonseed oil blended with different percentages of octanol and suspended MWCNT nanoparticles on diesel engine characteristics. J. Thermal Anal. Calorimetry 1–18.

Soudagar, M.E.M., Banapurmath, N.R., Afzal, A., Hossain, N., Abbas, M.M., Haniffa, M.A.C.M., et al., 2020b. Study of diesel engine characteristics by adding nanosized zinc oxide and diethyl ether additives in mahua biodiesel–diesel fuel blend. Sci. Rep. 10 (1), 15326.

Soudagar, M.E.M., Mujtaba, M.A., Safaei, M.R., Afzal, A., V, D.R., Ahmed, W., et al., 2021. Effect of Sr@ZnO nanoparticles and ricinus communis biodiesel-diesel fuel blends on modified CRDI diesel engine characteristics. Energy 215, 119094.

Soudagar, M.E.M., Nik-Ghazali, N.-N., Kalam, M.A., Badruddin, I.A., Banapurmath, N.R.a., 2019. The effects of graphene oxide nanoparticle additive stably dispersed in dairy scum oil biodiesel-diesel fuel blend on CI engine: performance, emission and combustion characteristics. Fuel 257, 116015.

Soudagar, M.E.M., Nik-Ghazali, N.-N., Kalam, M.Abul., Badruddin, I.A., Banapurmath, N.R., Akram, N., 2018. The effect of nano-additives in diesel-biodiesel fuel blends: A comprehensive review on stability, engine performance and emission characteristics. Energy Convers. Manage. 178, 146–177.

Sperring, T., Nowell, T., 2005. SYCLOPS—a qualitative debris classification system developed for RAF early failure detection centres. Tribol. Int. 38 (10), 898–903.

Sulek, M., Kulczycki, A., Malysa, A., 2010. Assessment of lubricity of compositions of fuel oil with biocomponents derived from rape-seed. Wear 268 (1–2), 104–108.

Venu, H., 2019. An experimental assessment on the influence of fuel-borne additives on ternary fuel (diesel–biodiesel–ethanol) blends operated in a single cylinder diesel engine. Environ. Sci. Pollut. Res. 26 (14), 14660–14672.

Wadumesthrige, K., Ara, M., Salley, S.O., Ng, K.Y.S., 2009. Investigation of Lubricity characteristics of Biodiesel in Petroleum and Synthetic Fuel. Energy Fuels 23 (4), 2229–2234.

Wu, Y., Tsui, W., Liu, T.J.W., 2007. Experimental analysis of tribological properties of lubricating oils with nanoparticle additives. 262 (7-8), 819–825.

Yusoff, M.N.A.M., Zulkifli, N.W.M., Sukiman, N.L., Chyuan, O.H., Hassan, M.H., Hasnul, M.H., et al., 2020. Sustainability of palm biodiesel in transportation: a review on biofuel standard, policy and international collaboration between Malaysia and Colombia. BioEnergy Res..

Zhang, Z., Lu, Y., Wang, Y., Yu, X., Smallbone, A., Dong, C., et al., 2019. Comparative study of using multi-wall carbon nanotube and two different sizes of cerium oxide nanopowders as fuel additives under various diesel engine conditions. Fuel 256, 115904.

Zulkifli, N.W.M., Kalam, M.A., Masjuki, H.H., Shahabuddin, M., Yunus, R., 2013. Wear prevention characteristics of a palm oil-based TMP (trimethylolpropane) ester as an engine lubricant. Energy 54, 167–173.